

Orthogonal and Biorthogonal $\sqrt{3}$ -refinement Wavelets for Hexagonal Data Processing

Qingtang Jiang

Abstract—The hexagonal lattice was proposed as an alternative method for image sampling. The hexagonal sampling has certain advantages over the conventionally used square sampling. Hence, the hexagonal lattice has been used in many areas.

A hexagonal lattice allows $\sqrt{3}$, dyadic and $\sqrt{7}$ refinements, which makes it possible to use the multiresolution (multiscale) analysis method to process hexagonally sampled data. The $\sqrt{3}$ -refinement is the most appealing refinement for multiresolution data processing due to the fact that it has the slowest progression through scale, and hence, it provides more resolution levels from which one can choose. This fact is the main motivation for the study of $\sqrt{3}$ -refinement surface subdivision, and it is also the main reason for the recommendation to use the $\sqrt{3}$ -refinement for discrete global grid systems. However, there is little work on compactly supported $\sqrt{3}$ -refinement wavelets. In this paper we study the construction of compactly supported orthogonal and biorthogonal $\sqrt{3}$ -refinement wavelets. In particular, we present a block structure of orthogonal FIR filter banks with 2-fold symmetry and construct the associated orthogonal $\sqrt{3}$ -refinement wavelets. We study the 6-fold axial symmetry of perfect reconstruction (biorthogonal) FIR filter banks. In addition, we obtain a block structure of 6-fold symmetric $\sqrt{3}$ -refinement filter banks and construct the associated biorthogonal wavelets.

Index Terms—Hexagonal lattice, hexagonal image, filter bank with 6-fold symmetry, $\sqrt{3}$ -refinement hexagonal filter bank, orthogonal $\sqrt{3}$ -refinement wavelet, biorthogonal $\sqrt{3}$ -refinement wavelet, $\sqrt{3}$ -refinement multiresolution decomposition/reconstruction.

EDICS Category: MRP-FBNK

I. INTRODUCTION

Images are conventionally sampled at the nodes on a square or rectangular lattice (array), and hence, traditional image processing is carried out on a square lattice. The hexagonal lattice (see the left part of Fig. 1) was proposed four decades ago as an alternative method for image sampling. The hexagonal sampling has certain advantages over the square sampling (see e.g. [1]–[8]), and it has been used in many areas [9]–[20].

For images/data sampled on a hexagonal lattice, each node on the hexagonal lattice represents a hexagonal cell with that node as its center. A node b and the hexagonal cell (called the elementary hexagonal cell) it represents are shown in the right part of Fig. 1. All the hexagonal elementary cells form a hexagonal tessellation of the plane.

It was shown in [21], [22] that a hexagonal lattice allows three interesting types of refinements: 3-size (3-branch, or

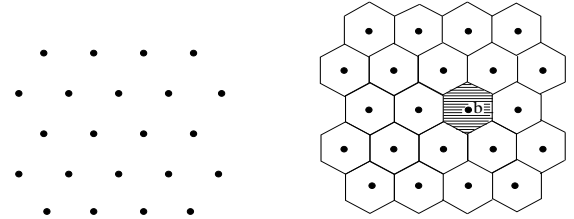


Fig. 1. Hexagonal lattice (left) and its associated hexagonal tessellation (right)

3-aperture), 4-size (4-branch, or 4-aperture) and 7-size (7-branch, or 7-aperture) refinements. In the left part of Fig. 2, the nodes with circles \circ form a new coarse lattice, which is called the 3-size (3-branch, or 3-aperture) sublattice of \mathcal{G} here, and it is denoted by \mathcal{G}_3 . From \mathcal{G} to \mathcal{G}_3 , the nodes are reduced by a factor $1/3$. So \mathcal{G}_3 is a coarse lattice of \mathcal{G} , and \mathcal{G} is a refinement of \mathcal{G}_3 . Since \mathcal{G}_3 is also a regular hexagonal lattice, we can repeat the same procedure to \mathcal{G}_3 , and we then have a high-order (coarse) regular hexagonal lattice with fewer nodes than \mathcal{G}_3 . Repeating this procedure, we have a set of lattices with fewer and fewer nodes. This set of lattices forms a “pyramid” or “tree” with a high-order lattice has fewer nodes than its predecessor by a factor of $1/3$. The hexagonal tessellation associated with \mathcal{G}_3 (nodes of \mathcal{G}_3 are the centroids of hexagons (with thick edges) to form the tessellation) is shown in the right picture of Fig. 2, where the hexagonal tessellation associated with \mathcal{G} (with thin hexagon edges) is also provided.

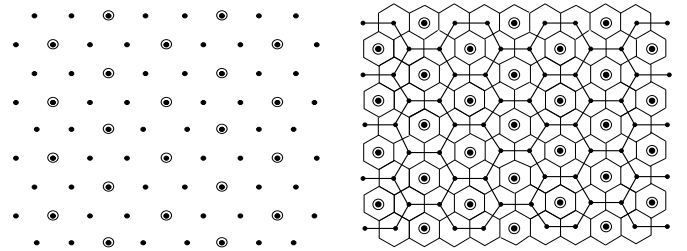


Fig. 2. Left: Hexagonal lattice \mathcal{G} (consisting of nodes \bullet) and its 3-size sublattice \mathcal{G}_3 (consisting of nodes \circ); Right: Hexagonal tessellations associated with \mathcal{G} and \mathcal{G}_3

Notice that the distance between any two (nearest) adjoint nodes in \mathcal{G}_3 is $\sqrt{3}$. Thus, the 3-size refinement is called $\sqrt{3}$ refinement in the area of Computer Aided Geometry Design [23]–[29], while they are called aperture 3 (refinement) in discrete global grid systems in [20].

The refinements of the hexagonal lattice allow the multiresolution (multiscale) analysis method to be used to process hexagonally sampled data. The dyadic (4-size) refinement is

Manuscript received December, 2008; revised May, 2009. The associate editor coordinating the review of this manuscript and approving it for publication was Dr. Gerald Schuller.

Q. Jiang is with the Department of Mathematics and Computer Science, University of Missouri–St. Louis, St. Louis, MO 63121, USA, e-mail: jiangq@umsl.edu, web: <http://www.cs.umsl.edu/~jiang>.

the most commonly used refinement for multiresolution image processing, and there are many papers on the construction and/or applications of dyadic hexagonal filter banks and wavelets, see e.g. [11], [12], [18], [30]-[36]. Though $\sqrt{7}$ -refinement (7-size refinement) has some special properties, the $\sqrt{7}$ -refinement multiresolution data processing results in a reduction in resolution by a factor 7 which may be too coarse and is undesirable. The reader refers to [37] for the construction of compactly supported $\sqrt{7}$ -refinement wavelets.

The $\sqrt{3}$ (3-size) refinement is the most appealing refinement for multiresolution data processing due to the fact that $\sqrt{3}$ -refinement has the slowest progression through scale and, hence, it gives applications more resolution levels from which to choose. This fact is the main motivation for the study of $\sqrt{3}$ -refinement subdivision in [23]-[29] and it is also the main reason for the recommendation to use the $\sqrt{3}$ -refinement for discrete global grid systems in [20], where $\sqrt{3}$ -refinement is called 3 aperture. The $\sqrt{3}$ -refinement has been used by engineers and scientists of the PYXIS innovation Inc. to develop The PYXIS Digital Earth Reference Model [38]. However, there is little work on $\sqrt{3}$ -refinement wavelets. [39], [40] are the only articles available in the literature on this topic. The authors of [39] construct $\sqrt{3}$, dyadic and $\sqrt{7}$ refinement complex pre-wavelets (semi-orthogonal wavelets) on the hexagonal lattice with the scaling functions being the elementary polyharmonic hexagonal B-splines introduced in [39]. Though their filters are not FIR, the wavelets in [39] have a very nice property that they are rotation-covariant. (The reader refers to [41] for rotation covariant quincunx wavelets on the square lattice.) The authors of [40] construct compactly supported biorthogonal $\sqrt{3}$ -refinement wavelets by adopting the method in [34] for the construction of dyadic wavelets. The wavelets in [34] and [40] are constructed for the purpose of surface multiresolution processing which involves both regular and extraordinary nodes (vertices) in the surfaces. It is hard to calculate the L^2 inner product of the scaling functions (also called basis functions) and wavelets associated with extraordinary nodes. Thus, when considering the biorthogonality, [34] and [40] do not use the L^2 inner product. Instead, they use a “discrete inner product” related to the discrete filters. That discrete inner product may result in basis functions and wavelets which are not $L^2(\mathbb{R}^2)$ functions. Indeed, the $\sqrt{3}$ -refinement analysis basis functions and wavelets (even associated with regular nodes) constructed in [40] are not in $L^2(\mathbb{R}^2)$, and hence they cannot generate Riesz bases for $L^2(\mathbb{R}^2)$. In this paper we study the construction of compactly supported orthogonal and biorthogonal $\sqrt{3}$ -refinement wavelets (for regular nodes) with the conventional L^2 inner product.

The rest of this paper is organized as follows. In §II, we provide $\sqrt{3}$ -refinement multiresolution algorithms and some basic results on the orthogonality/biorthogonality of $\sqrt{3}$ -refinement filter banks. In §III, we study the construction of compactly supported orthogonal $\sqrt{3}$ -refinement wavelets. In §IV, we address the construction of $\sqrt{3}$ -refinement perfect reconstruction (biorthogonal) filter banks with 6-fold axial symmetry and the associated biorthogonal wavelets.

In this paper we use bold-faced letters such as $\mathbf{k}, \mathbf{x}, \omega$ to

denote elements of \mathbf{Z}^2 and \mathbb{R}^2 . A multi-index \mathbf{k} of \mathbf{Z}^2 and a point \mathbf{x} in \mathbb{R}^2 will be written as row vectors

$$\mathbf{k} = (k_1, k_2), \mathbf{x} = (x_1, x_2).$$

However, \mathbf{k} and \mathbf{x} should be understood as column vectors $[k_1, k_2]^T$ and $[x_1, x_2]^T$ when we consider $A\mathbf{k}$ and $A\mathbf{x}$, where A is a 2×2 matrix. For a matrix M , we use M^* to denote its complex conjugate and transpose \overline{M}^T , and for a nonsingular matrix M , M^{-T} denotes $(M^{-1})^T$.

II. MULTIREOLUTION PROCESSING WITH $\sqrt{3}$ -REFINEMENT FILTER BANKS

In this section, we review $\sqrt{3}$ -refinement multiresolution algorithms and some basic results on the orthogonality/biorthogonality of $\sqrt{3}$ -refinement filter banks.

Let \mathcal{G} denote the regular unit hexagonal lattice defined by

$$\mathcal{G} = \{k_1 \mathbf{v}_1 + k_2 \mathbf{v}_2 : k_1, k_2 \in \mathbf{Z}\}, \quad (1)$$

where

$$\mathbf{v}_1 = [1, 0]^T, \mathbf{v}_2 = [-1/2, \sqrt{3}/2]^T.$$

To a node $\mathbf{g} = k_1 \mathbf{v}_1 + k_2 \mathbf{v}_2$ of \mathcal{G} , we use (k_1, k_2) to indicate \mathbf{g} , see the left part of Fig. 3 for the labelling of \mathcal{G} . Thus, for hexagonal data c sampled on \mathcal{G} , instead of using $c_{\mathbf{g}}$, we use c_{k_1, k_2} to denote the pixel of c at $\mathbf{g} = k_1 \mathbf{v}_1 + k_2 \mathbf{v}_2$. Therefore, we write c , data hexagonally sampled on \mathcal{G} , as $c = \{c_{k_1, k_2}\}_{k_1, k_2 \in \mathbf{Z}}$, see the right part of Fig. 3 for c_{k_1, k_2} .

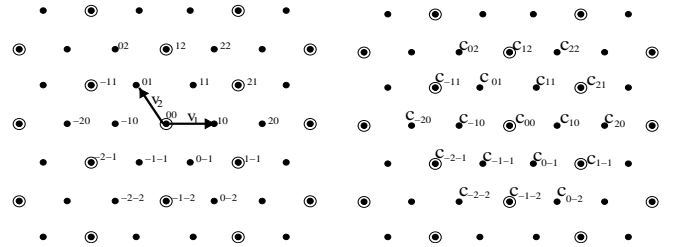


Fig. 3. Left: Indices for hexagonal nodes; Right: Indices for hexagonally sampled data c

Denote $\mathbf{V}_1 = 2\mathbf{v}_1 + \mathbf{v}_2$, $\mathbf{V}_2 = -\mathbf{v}_1 + \mathbf{v}_2$. Then the coarse lattice \mathcal{G}_3 is generated by \mathbf{V}_1 and \mathbf{V}_2 :

$$\mathcal{G}_3 = \{k_1 \mathbf{V}_1 + k_2 \mathbf{V}_2 : k_1, k_2 \in \mathbf{Z}\}.$$

Observe that $k_1 \mathbf{V}_1 + k_2 \mathbf{V}_2 = (2k_1 - k_2)\mathbf{v}_1 + (k_1 + k_2)\mathbf{v}_2$. Thus, the indices for nodes of \mathcal{G}_3 are $\{(2k_1 - k_2, k_1 + k_2), k_1, k_2 \in \mathbf{Z}\}$ and hence, the data c associated with \mathcal{G}_3 is given by $\{c_{(2k_1 - k_2, k_1 + k_2)}\}_{k_1, k_2 \in \mathbf{Z}}$.

To provide the multiresolution image decomposition and reconstruction algorithms, we need to choose a 2×2 matrix M , called the *dilation matrix*, such that it maps the indices for the nodes of \mathcal{G} onto those for the nodes of the coarse lattice \mathcal{G}_3 , namely, we need to choose M such that

$$M : (k_1, k_2) \rightarrow (2k_1 - k_2, k_1 + k_2), k_1, k_2 \in \mathbf{Z}.$$

One may choose M to be a matrix that maps $A = \{(1, 0), (1, 1), (0, 1), (-1, 0), (-1, -1), (0, -1)\}$ onto $B = \{(2, 1), (1, 2), (-1, 1), (-2, -1), (-1, -2), (1, -1)\}$. Notice that $k_1 \mathbf{v}_1 + k_2 \mathbf{v}_2$ with $(k_1, k_2) \in A$ form a hexagon,

while $k_1\mathbf{v}_1 + k_2\mathbf{v}_2$ with $(k_1, k_2) \in B$ form a hexagon with vertices in \mathcal{G}_3 . There are several choices for such a matrix M . Here we consider two of such matrices (refer to [28] for other choices of M):

$$M_1 = \begin{bmatrix} 2 & -1 \\ 1 & 1 \end{bmatrix}, \quad M_2 = \begin{bmatrix} 2 & -1 \\ 1 & -2 \end{bmatrix} \quad (2)$$

For a sequence $\{p_{\mathbf{k}}\}_{\mathbf{k} \in \mathbf{Z}^2}$ of real numbers with finitely many $p_{\mathbf{k}}$ nonzero, let $p(\boldsymbol{\omega})$ denote the finite impulse response (FIR) filter with its impulse response coefficients $p_{\mathbf{k}}$ (here a factor $1/3$ is added for convenience):

$$p(\boldsymbol{\omega}) = (1/3) \sum_{\mathbf{k} \in \mathbf{Z}^2} p_{\mathbf{k}} e^{-i\mathbf{k} \cdot \boldsymbol{\omega}}.$$

When $\mathbf{k}, \mathbf{k}' \in \mathbf{Z}^2$, are considered as indices for nodes $\mathbf{g} = k_1\mathbf{v}_1 + k_2\mathbf{v}_2$ of \mathcal{G} , $p(\boldsymbol{\omega})$ is a hexagonal filter, see Fig. 4 for the coefficients p_{k_1, k_2} . In this paper, a filter means a hexagonal filter though the indices of its coefficients are given by \mathbf{k} with \mathbf{k} in the square lattice \mathbf{Z}^2 .

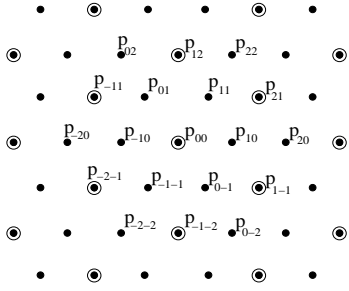


Fig. 4. Indices for impulse response coefficients p_{k_1, k_2}

For a pair of filter banks $\{p, q^{(1)}, q^{(2)}\}$ and $\{\tilde{p}, \tilde{q}^{(1)}, \tilde{q}^{(2)}\}$, the multiresolution decomposition algorithm with a dilation matrix M for an input hexagonally sampled image $c_{\mathbf{k}}^0$ is

$$\begin{cases} c_{\mathbf{n}}^{j+1} = (1/3) \sum_{\mathbf{k} \in \mathbf{Z}^2} p_{\mathbf{k}-M\mathbf{n}} c_{\mathbf{k}}^j, \\ d_{\mathbf{n}}^{(\ell, j+1)} = (1/3) \sum_{\mathbf{k} \in \mathbf{Z}^2} q_{\mathbf{k}-M\mathbf{n}}^{(\ell)} c_{\mathbf{k}}^j, \end{cases} \quad (3)$$

with $\ell = 1, 2, \mathbf{n} \in \mathbf{Z}^2$ for $j = 0, 1, \dots, J-1$, and the multiresolution reconstruction algorithm is given by

$$\hat{c}_{\mathbf{k}}^j = \sum_{\mathbf{n} \in \mathbf{Z}^2} \tilde{p}_{\mathbf{k}-M\mathbf{n}} \hat{c}_{\mathbf{n}}^{j+1} + \sum_{1 \leq \ell \leq 2} \sum_{\mathbf{n} \in \mathbf{Z}^2} \tilde{q}_{\mathbf{k}-M\mathbf{n}}^{(\ell)} d_{\mathbf{n}}^{(\ell, j+1)} \quad (4)$$

with $\mathbf{k} \in \mathbf{Z}^2$ for $j = J-1, J-2, \dots, 0$, where $\hat{c}_{\mathbf{n}, J} = c_{\mathbf{n}, J}$. We say hexagonally filter banks $\{p, q^{(1)}, q^{(2)}\}$ and $\{\tilde{p}, \tilde{q}^{(1)}, \tilde{q}^{(2)}\}$ to be the *perfect reconstruction (PR) filter banks* if $\hat{c}_{\mathbf{k}}^j = c_{\mathbf{k}}^j$, $0 \leq j \leq J-1$ for any input hexagonally sampled image $c_{\mathbf{k}}^0$. $\{p, q^{(1)}, q^{(2)}\}$ is called the *analysis filter bank* and $\{\tilde{p}, \tilde{q}^{(1)}, \tilde{q}^{(2)}\}$ the *synthesis filter bank*.

From (3) and (4), we know when the indices of hexagonally sampled data are labelled by $(k_1, k_2) \in \mathbf{Z}^2$ as in Fig. 3, the decomposition and reconstruction algorithms for hexagonal data with hexagonal filter banks are the conventional multiresolution decomposition and reconstruction algorithms for squarely sampled images. Thus, $\{p, q^{(1)}, q^{(2)}\}$ and $\{\tilde{p}, \tilde{q}^{(1)}, \tilde{q}^{(2)}\}$ are

PR filter banks if and only if

$$\sum_{0 \leq k \leq 2} p(\boldsymbol{\omega} + 2\pi M^{-T} \boldsymbol{\eta}_k) \overline{\tilde{p}(\boldsymbol{\omega} + 2\pi M^{-T} \boldsymbol{\eta}_k)} = 1 \quad (5)$$

$$\sum_{0 \leq k \leq 2} p(\boldsymbol{\omega} + 2\pi M^{-T} \boldsymbol{\eta}_k) \overline{\tilde{q}^{(\ell)}(\boldsymbol{\omega} + 2\pi M^{-T} \boldsymbol{\eta}_k)} = 0 \quad (6)$$

$$\sum_{0 \leq k \leq 2} q^{(\ell')}(\boldsymbol{\omega} + 2\pi M^{-T} \boldsymbol{\eta}_k) \overline{\tilde{q}^{(\ell)}(\boldsymbol{\omega} + 2\pi M^{-T} \boldsymbol{\eta}_k)} = \delta_{\ell' - \ell}, \quad (7)$$

for $1 \leq \ell, \ell' \leq 2$, $\boldsymbol{\omega} \in \mathbb{R}^2$, where $\boldsymbol{\eta}_j$, $0 \leq j \leq 2$ are the representatives of the group $\mathbf{Z}^2/(M^T \mathbf{Z}^2)$, δ_k is the kronecker-delta sequence: $\delta_k = 1$ if $k = 0$, and $\delta_k = 0$ if $k \neq 0$. When M is the dilation matrix M_1 or M_2 in (2), we may choose $\boldsymbol{\eta}_j$, $0 \leq j \leq 2$ to be

$$\boldsymbol{\eta}_0 = (0, 0), \boldsymbol{\eta}_1 = (1, 0), \boldsymbol{\eta}_2 = (-1, 0). \quad (8)$$

Filter banks $\{p, q^{(1)}, q^{(2)}\}$ and $\{\tilde{p}, \tilde{q}^{(1)}, \tilde{q}^{(2)}\}$ are also said to be *biorthogonal* if they satisfy (5)-(7); and a filter bank $\{p, q^{(1)}, q^{(2)}\}$ is said to be *orthogonal* if it satisfies (5)-(7) with $\tilde{p} = p$, $\tilde{q}^{(\ell)} = q^{(\ell)}$, $1 \leq \ell \leq 2$.

Let $\{p, q^{(1)}, q^{(2)}\}$ and $\{\tilde{p}, \tilde{q}^{(1)}, \tilde{q}^{(2)}\}$ be a pair of FIR filter banks. Let ϕ and $\tilde{\phi}$ be the scaling functions (with dilation matrix M) associated with lowpass filters $p(\boldsymbol{\omega})$ and $\tilde{p}(\boldsymbol{\omega})$ respectively, namely, $\phi, \tilde{\phi}$ satisfy the refinement equations:

$$\phi(\mathbf{x}) = \sum_{\mathbf{k} \in \mathbf{Z}^2} p_{\mathbf{k}} \phi(M\mathbf{x} - \mathbf{k}), \quad \tilde{\phi}(\mathbf{x}) = \sum_{\mathbf{k} \in \mathbf{Z}^2} \tilde{p}_{\mathbf{k}} \tilde{\phi}(M\mathbf{x} - \mathbf{k}), \quad (9)$$

and $\psi^{(\ell)}, \tilde{\psi}^{(\ell)}$, $1 \leq \ell \leq 2$ are given by

$$\begin{aligned} \psi^{(\ell)}(\mathbf{x}) &= \sum_{\mathbf{k} \in \mathbf{Z}^2} q_{\mathbf{k}}^{(\ell)} \phi(M\mathbf{x} - \mathbf{k}), \\ \tilde{\psi}^{(\ell)}(\mathbf{x}) &= \sum_{\mathbf{k} \in \mathbf{Z}^2} \tilde{q}_{\mathbf{k}}^{(\ell)} \tilde{\phi}(M\mathbf{x} - \mathbf{k}), \end{aligned} \quad (10)$$

where $p_{\mathbf{k}}, \tilde{p}_{\mathbf{k}}, q_{\mathbf{k}}^{(\ell)}, \tilde{q}_{\mathbf{k}}^{(\ell)}$ are the impulse response coefficients of $p(\boldsymbol{\omega}), \tilde{p}(\boldsymbol{\omega}), q^{(\ell)}(\boldsymbol{\omega}), \tilde{q}^{(\ell)}(\boldsymbol{\omega})$, respectively

If $\{p, q^{(1)}, q^{(2)}\}$ and $\{\tilde{p}, \tilde{q}^{(1)}, \tilde{q}^{(2)}\}$ are biorthogonal to each other (with dilation M), then under certain mild conditions (see e.g. [42], [43], [44]), ϕ and $\tilde{\phi}$ are biorthogonal duals:

$\int_{\mathbb{R}^2} \phi(\mathbf{x}) \tilde{\phi}(\mathbf{x} - \mathbf{k}) d\mathbf{x} = \delta_{\mathbf{k}}$, $\mathbf{k} \in \mathbf{Z}^2$, where $\delta_{\mathbf{k}} = \delta_{k_1} \delta_{k_2}$. In this case, $\psi^{(\ell)}, \tilde{\psi}^{(\ell)}$, $\ell = 1, 2$, are biorthogonal wavelets, namely, $\{\psi_{j, \mathbf{k}}^{(\ell)} : \ell = 1, 2, j \in \mathbf{Z}, \mathbf{k} \in \mathbf{Z}^2\}$ and $\{\tilde{\psi}_{j, \mathbf{k}}^{(\ell)} : \ell = 1, 2, j \in \mathbf{Z}, \mathbf{k} \in \mathbf{Z}^2\}$ are Riesz bases of $L^2(\mathbb{R}^2)$ and they are biorthogonal to each other:

$$\int_{\mathbb{R}^2} \psi_{j, \mathbf{k}}^{(\ell)}(\mathbf{x}) \overline{\tilde{\psi}_{j', \mathbf{k}'}^{(\ell')}}(\mathbf{x}) d\mathbf{x} = \delta_{j-j'} \delta_{\ell-\ell'} \delta_{\mathbf{k}-\mathbf{k}'},$$

for $j, j' \in \mathbf{Z}$, $1 \leq \ell, \ell' \leq 2$, $\mathbf{k}, \mathbf{k}' \in \mathbf{Z}^2$, where

$$\psi_{j, \mathbf{k}}^{(\ell)}(\mathbf{x}) = 3^{j/2} \psi^{(\ell)}(M^j \mathbf{x} - \mathbf{k}), \quad \tilde{\psi}_{j, \mathbf{k}}^{(\ell)}(\mathbf{x}) = 3^{j/2} \tilde{\psi}^{(\ell)}(M^j \mathbf{x} - \mathbf{k}).$$

Remark 1: One can verify that $\{M_1^{-T} \boldsymbol{\eta}_j : j = 0, 1, 2\} = \{M_2^{-T} \boldsymbol{\eta}_j : j = 0, 1, 2\}$, where $\boldsymbol{\eta}_j$, $j = 0, 1, 2$ are the representatives for both $\mathbf{Z}^2/M_1^T \mathbf{Z}^2$ and $\mathbf{Z}^2/M_2^T \mathbf{Z}^2$ given in (8). Thus, $\{p, q^{(1)}, q^{(2)}\}$ and $\{\tilde{p}, \tilde{q}^{(1)}, \tilde{q}^{(2)}\}$ are biorthogonal with one of M_1, M_2 , say M_1 , then they are also biorthogonal to each other with the other dilation matrix, M_2 .

ϕ and $\tilde{\phi}$ are refinable functions along \mathbf{Z}^2 . $\phi, \tilde{\phi}$ and $\psi^{(\ell)}, \tilde{\psi}^{(\ell)}, \ell = 1, 2$ are the conventional scaling functions and wavelets. Let U be the matrix defined by

$$U = \begin{bmatrix} 1 & \sqrt{3}/3 \\ 0 & 2\sqrt{3}/3 \end{bmatrix}.$$

Then U transforms the regular unit hexagonal lattice \mathcal{G} onto the square lattice \mathbf{Z}^2 . Define

$$\begin{aligned} \Phi(\mathbf{x}) &= \phi(U\mathbf{x}), \quad \Psi^{(\ell)}(\mathbf{x}) = \psi^{(\ell)}(U\mathbf{x}), \\ \tilde{\Phi}(\mathbf{x}) &= \tilde{\phi}(U\mathbf{x}), \quad \tilde{\Psi}^{(\ell)}(\mathbf{x}) = \tilde{\psi}^{(\ell)}(U\mathbf{x}), \ell = 1, 2. \end{aligned} \quad (11)$$

Then Φ and $\tilde{\Phi}$ are refinable along \mathcal{G} with the same coefficients $p_{\mathbf{k}}$ and $\tilde{p}_{\mathbf{k}}$ for ϕ and $\tilde{\phi}$, and $\Psi^{(\ell)}$ and $\tilde{\Psi}^{(\ell)}, \ell = 1, 2$ are hexagonal biorthogonal wavelets (along the hexagonal lattice \mathcal{G}).

In the rest of this section, we give the definitions of the symmetries of filter banks considered in this paper.

Definition 1: A hexagonal filter bank $\{p, q^{(1)}, q^{(2)}\}$ is said to have 2-fold rotational symmetry if p is invariant under π rotation, and $q^{(2)}$ is the π rotation of $q^{(1)}$.

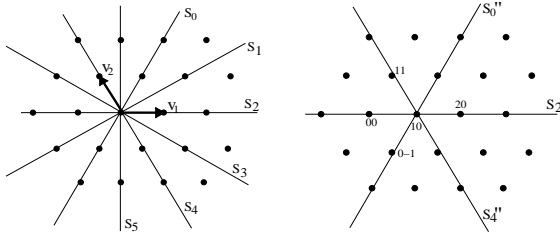


Fig. 5. Left: 6 axes (lines) of symmetry for lowpass filter p ; Right: 3 axes (lines) of symmetry for highpass filter $q^{(1)}$

Definition 2: Let $S_j, 0 \leq j \leq 5$ be the axes on the left of Fig. 5. A hexagonal filter bank $\{p, q^{(1)}, q^{(2)}\}$ is said to have 6-fold axial symmetry or 6-fold line symmetry if (i) p is symmetric around S_0, \dots, S_5 , (ii) $e^{-i\omega_1} q^{(1)}(\omega)$ is symmetric around S_0, S_2, S_4 , and (iii) $q^{(2)}$ is the π rotation of $q^{(1)}$.

The right part of Fig. 5 shows the symmetry of $q^{(1)}$, namely, $q^{(1)}$ is symmetric around the axes S_0'', S_2'', S_4'' , where S_0'' and S_4'' are the 1-unit right shifts of S_0 and S_4 respectively.

The symmetry of hexagonal filter banks is important for image/data processing, and it leads to simpler algorithms and efficient computations. Unlike the orthogonal dyadic refinement and $\sqrt{7}$ -refinement hexagonal filter banks which may have 3-fold and 6-fold symmetry respectively, it seems hard to construct orthogonal $\sqrt{3}$ -refinement filter banks with high symmetry (only 2-fold symmetry can be obtained here). While for biorthogonal filter banks, we have more flexibility for their construction and very high symmetry can be gained. Some 3-direction box-splines in [45] are symmetric around $S_j, 0 \leq j \leq 5$, and such box-splines are called to have the *full set of symmetries*. For the biorthogonal filter banks considered in this paper, the lowpass filters have the full set of symmetries, and the highpass filters also have certain symmetry as well. Such a symmetry of our filter banks not only results in efficient computations, but also makes it possible to design surface multiresolution algorithms for extraordinary nodes when the

filters constructed in this paper are used for the multiresolution algorithms for regular nodes.

In the next two sections, we discuss the construction of 2-fold symmetric orthogonal and 6-fold symmetric biorthogonal $\sqrt{3}$ -refinement wavelets. When we consider orthogonal and biorthogonal wavelets, from Remark 1, we need only to consider one of the dilation matrices M_1, M_2 . In the rest of this paper, without loss of generality, we choose M to be M_1 .

III. ORTHOGONAL $\sqrt{3}$ -REFINEMENT WAVELETS

In this section we construct compactly supported orthogonal $\sqrt{3}$ -refinement wavelets with 2-fold rotational symmetry. First we give a family of 2-fold symmetric filter banks.

By the definition of the symmetry, we know that an FIR filter bank $\{p, q^{(1)}, q^{(2)}\}$ has 2-fold rotational symmetry if and only if $p_{-\mathbf{k}} = p_{\mathbf{k}}, q_{\mathbf{k}}^{(2)} = q_{-\mathbf{k}}^{(1)}, \mathbf{k} \in \mathbf{Z}^2$, namely,

$$p(-\omega) = p(\omega), \quad q^{(2)}(\omega) = q^{(1)}(-\omega), \quad \omega \in \mathbb{R}^2,$$

or equivalently,

$$\begin{aligned} [p, q^{(1)}, q^{(2)}]^T(-\omega) \\ = M_0 [p(\omega), q^{(1)}(\omega), q^{(2)}(\omega)]^T, \end{aligned} \quad (12)$$

where

$$M_0 = \begin{bmatrix} 1 & 0 & 0 \\ 0 & 0 & 1 \\ 0 & 1 & 0 \end{bmatrix}.$$

We hope to construct filter banks $\{p, q^{(1)}, q^{(2)}\}$ given by the product of appropriate block matrices. If we can write a symmetric FIR filter bank $[p(\omega), q^{(1)}(\omega), q^{(2)}(\omega)]^T$ as a product $B(M^T \omega)[p_s(\omega), q_s^{(1)}(\omega), q_s^{(2)}(\omega)]^T$, where M is M_1 defined in (2), $B(\omega)$ is a 3×3 matrix whose entries are trigonometric polynomials, and $\{p_s, q_s^{(1)}, q_s^{(2)}\}$ is another FIR filter bank with 2-fold rotational symmetry, then (12) implies that $B(\omega)$ satisfies

$$B(-M^T \omega) = M_0 B(M^T \omega) M_0^{-1}. \quad (13)$$

Denote

$$I_0(\omega) = [1, e^{-i\omega_1}, e^{i\omega_1}]^T. \quad (14)$$

Clearly, $I_0(\omega)$ satisfies (12). Therefore, 1-tap filter bank $\{1, e^{-i\omega_1}, e^{i\omega_1}\}$ has 2-fold rotational symmetry, and it could be used as the initial symmetric filter bank.

Denote

$$\begin{aligned} D_1(\omega) &= \text{diag}(1, e^{-i\omega_2}, e^{i\omega_2}), \\ D_2(\omega) &= \text{diag}(1, e^{-i(\omega_1+\omega_2)}, e^{i(\omega_1+\omega_2)}), \\ D_3(\omega) &= \text{diag}(1, e^{-i\omega_1}, e^{i\omega_1}). \end{aligned} \quad (15)$$

Then one can easily verify that $D_j(\omega), D_j(-\omega), j = 1, 2, 3$ satisfy (13), and thus they could be used to build the block matrices. Next we use $B(\omega) = BD(\omega)$ as the block matrix, where B is a 3×3 (real) constant matrix, and $D(\omega)$ is $D_j(\omega)$ or $D_j(-\omega)$ for some $j, 1 \leq j \leq 3$. Based on the above discussion, we know that $B(\omega) = BD(\omega)$ satisfies (13) if and only if B satisfies $M_0 B M_0^{-1} = B$, which is equivalent to that B has the form:

$$B = \begin{bmatrix} b_{11} & b_{12} & b_{12} \\ b_{21} & b_{22} & b_{23} \\ b_{21} & b_{23} & b_{22} \end{bmatrix}. \quad (16)$$

Thus we conclude that if $\{p, q^{(1)}, q^{(2)}\}$ is given by

$$\begin{aligned} & [p(\omega), q^{(1)}(\omega), q^{(2)}(\omega)]^T = \\ & (1/\sqrt{3})B_n D(M^T \omega) \cdots B_1 D(M^T \omega) B_0 I_0(\omega) \end{aligned} \quad (17)$$

where $n \in \mathbf{Z}_+$, $I_0(\omega)$ is defined by (14), $B_k, 0 \leq k \leq n$ are constant matrices of the form (16), and each $D(\omega)$ is $D_j(\omega)$ or $D_j(-\omega)$ for some $j, 1 \leq j \leq 3$, then $\{p, q^{(1)}, q^{(2)}\}$ is an FIR filter bank with 2-fold rotational symmetry.

Next, we show that the block structure in (17) yields 2-fold symmetric orthogonal FIR filter banks.

For an FIR filter bank $\{p, q^{(1)}, q^{(2)}\}$, denote $q^{(0)}(\omega) = p(\omega)$. Let $U(\omega)$ be a 3×3 matrix defined by $U(\omega) = [q^{(\ell)}(\omega + \eta_j)]_{0 \leq \ell, j \leq 2}$, where η_0, η_1, η_2 are given in (8). Then $\{p, q^{(1)}, q^{(2)}\}$ is orthogonal if $U(\omega)$ is unitary for all $\omega \in \mathbb{R}^2$, that is it satisfies

$$U(\omega)U(\omega)^* = I_3, \quad \omega \in \mathbb{R}^2. \quad (18)$$

Write $q^{(\ell)}(\omega), 0 \leq \ell \leq 2$ as

$$\begin{aligned} q^{(\ell)}(\omega) &= (1/\sqrt{3})(q_0^{(\ell)}(M^T \omega) + q_1^{(\ell)}(M^T \omega)e^{-i\omega_1} \\ &\quad + q_2^{(\ell)}(M^T \omega)e^{i\omega_1}), \end{aligned}$$

where $q_k^{(\ell)}(\omega)$ are trigonometric polynomials. Let $V(\omega)$ denote the polyphase matrix (with dilation matrix M) of $\{p(\omega), q^{(1)}(\omega), q^{(2)}(\omega)\}$:

$$V(\omega) = \begin{bmatrix} p_0(\omega) & p_1(\omega) & p_2(\omega) \\ q_0^{(1)}(\omega) & q_1^{(1)}(\omega) & q_2^{(1)}(\omega) \\ q_0^{(2)}(\omega) & q_1^{(2)}(\omega) & q_2^{(2)}(\omega) \end{bmatrix}. \quad (19)$$

From the fact that

$$[p(\omega), q^{(1)}(\omega), q^{(2)}(\omega)]^T = (1/\sqrt{3})V(M^T \omega)I_0(\omega),$$

where $I_0(\omega)$ is defined by (14), and that the 3×3 matrix $(1/\sqrt{3})[I_0(\omega + 2\pi M^{-T}\eta_0), I_0(\omega + 2\pi M^{-T}\eta_1), I_0(\omega + 2\pi M^{-T}\eta_2)]$ is unitary for all $\omega \in \mathbb{R}^2$, we know that (18) holds if and only if $V(\omega)$ is unitary for all $\omega \in \mathbb{R}^2$.

If $\{p, q^{(1)}, q^{(2)}\}$ is given by (17), then its polyphase matrix $V(\omega)$ is $V(\omega) = B_n D(\omega) B_{n-1} D(\omega) \cdots B_1 D(\omega) B_0$. Since each $D(\omega)$ is unitary, we know that if constant matrices $B_k, 0 \leq k \leq n$, are orthogonal, then $V(\omega)$ is unitary.

Next, we consider the orthogonality of a matrix B of the form (16). To this regard, let U denote the unitary matrix:

$$U = \begin{bmatrix} 1 & 0 & 0 \\ 0 & 1/\sqrt{2} & 1/\sqrt{2} \\ 0 & 1/\sqrt{2} & -1/\sqrt{2} \end{bmatrix}.$$

Then

$$UBU^* = \begin{bmatrix} b_{11} & \sqrt{2}b_{12} & 0 \\ \sqrt{2}b_{21} & b_{22} + b_{23} & 0 \\ 0 & 0 & b_{22} - b_{23} \end{bmatrix}.$$

Thus B is orthogonal if and only if $\begin{bmatrix} b_{11} & \sqrt{2}b_{12} \\ \sqrt{2}b_{21} & b_{22} + b_{23} \end{bmatrix}$ is orthogonal and $b_{22} + b_{23} = \pm 1$, which implies that b_{ij} can be written as

$$\begin{aligned} b_{11} &= s_0 \cos \theta, \quad b_{12} = (1/\sqrt{2}) \sin \theta, \quad b_{21} = (1/\sqrt{2}) s_0 \sin \theta, \\ b_{22} + b_{23} &= -\cos \theta, \quad b_{22} - b_{23} = s_1, \end{aligned} \quad (20)$$

where $s_0 = \pm 1, s_1 = \pm 1, \theta \in \mathbb{R}$. Thus an orthogonal matrix B of the form (16) has one parameter. If we choose $s_0 = 1, s_1 = 1$ and write $\cos \theta = (1 - t^2)/(1 + t^2)$, $\sin \theta = (2t)/(1 + t^2)$, then we have

$$b_{11} = \frac{1-t^2}{1+t^2}, \quad b_{12} = b_{21} = \frac{\sqrt{2}t}{1+t^2}, \quad b_{22} = \frac{t^2}{1+t^2}, \quad b_{23} = \frac{1}{1+t^2}. \quad (21)$$

We have therefore the following theorem.

Theorem 1: Suppose $\{p, q^{(1)}, q^{(2)}\}$ is given by (17). If each $B_k, 0 \leq k \leq n$ is of the form (16) and its entries b_{ij} are given by (20) for some θ_k , then $\{p, q^{(1)}, q^{(2)}\}$ is an orthogonal FIR filter bank with 2-fold rotational symmetry.

With such a family of orthogonal filter banks, by selecting the free parameters, one can design the filters with desirable properties. Here we consider the filters based on the Sobolev smoothness of the associated scaling functions ϕ . We say ϕ to be in the Sobolev space W^s for some $s > 0$ if ϕ satisfies $\int_{\mathbb{R}^2} (1 + |\omega|^2)^s |\hat{\phi}(\omega)|^2 d\omega < \infty$. To assure that $\phi \in W^s$, the associated FIR lowpass filter $p(\omega)$ has sum rules of certain order. $p(\omega)$ is said to have *sum rule order* m (with dilation matrix M) provided that $p(0, 0) = 1$ and

$$D_1^{\alpha_1} D_2^{\alpha_2} p(2\pi M^{-T} \eta_j) = 0, \quad j = 1, 2, \quad (22)$$

for all $(\alpha_1, \alpha_2) \in \mathbf{Z}_+^2$ with $\alpha_1 + \alpha_2 < m$, where $\eta_j, j = 1, 2$, are defined by (8), D_1 and D_2 denote the partial derivatives with the first and second variables of $p(\omega)$ respectively. The Sobolev smoothness of ϕ can be given by the eigenvalues of the so-called transition operator matrix T_p associated with the lowpass filter p , see [46], [47].

We find that if the orthogonal filter bank $\{p, q^{(1)}, q^{(2)}\}$ is given by (17) with $n = 0$ or $n = 1$, then the lowpass filter $p(\omega)$ cannot achieve sum rule order 2, and hence, the smoothness order of ϕ is very low. In the following two examples, we consider the filter banks with $n = 2$ and $n = 3$.

Example 1: Let $\{p, q^{(1)}, q^{(2)}\}$ be the orthogonal filter bank with 2-fold rotational symmetry given by (17) for $n = 2$: $B_2 D_2(M^T \omega) B_1 D_1(M^T \omega) B_0 I_0(\omega)$, where D_1, D_2 are defined in (15), B_0, B_1 and B_2 are orthogonal matrices of the form (16) with their entries b_{ij} given by (21) for parameters t_0, t_1 and t_2 . The lowpass filter $p(\omega)$ depends on these three parameters t_0, t_1 and t_2 . By solving the system of equations for sum rule order 2, we get

$$\begin{aligned} t_0 &= -(\sqrt{2}/2)(3 + \sqrt{19}), \quad t_1 = (\sqrt{2}/6)(-5 + \sqrt{19}), \\ t_2 &= -(\sqrt{2}/2)(5 + 3\sqrt{3}). \end{aligned}$$

The resulting scaling function ϕ with $M = M_1$ is in $W^{0.79282}$. The resulting coefficients $p_k, q_k^{(1)}, q_k^{(2)}$ and the pictures for ϕ and $\psi^{(1)}$ are provided in the long version of this paper downloadable at author's web site.

From Remark 1, this resulting filter bank is orthogonal with dilation matrix M_2 . Furthermore, one can verify that the resulting $p(\omega)$ also has sum rule order 2 with M_2 , and the associated scaling function (with M_2) is in $W^{0.80115}$. \diamond

Example 2: Let $\{p, q^{(1)}, q^{(2)}\}$ be the orthogonal filter bank with 2-fold rotational symmetry given by (17) for $n = 3$: $B_3 D_1(M^T \omega) B_2 D_2(M^T \omega) B_1 D_1(M^T \omega) B_0 I_0(\omega)$, where D_1, D_2 are defined in (15), B_0, B_1, B_2 and B_3 are orthogonal

matrices of the form (16) with their entries b_{ij} given by (21) for parameters t_0, t_1, t_2 and t_3 . If we choose,

$$t_0 = -3.96188283176253, \quad t_1 = -0.09286132100086, \\ t_2 = -5.26430640532092, \quad t_3 = 0.04994199850331,$$

then the resulting $p(\omega)$ has sum rule order 2 (with both M_1 and M_2). The corresponding scaling function ϕ with $M = M_1$ is in $W^{0.84094}$, and that with $M = M_2$ is in $W^{1.06523}$. \diamond

The orthogonal FIR filter banks given by (17) with more blocks $B_k D(M^T \omega)$ will produce wavelets with small increments of smoothness order. Similar to orthogonal dyadic refinement and $\sqrt{7}$ -refinement hexagonal wavelets, we find it is also hard to construct orthogonal $\sqrt{3}$ -refinement wavelets with high smoothness order. In the next section, we consider biorthogonal filter banks, which give us some flexibility for the construction of PR filter banks.

In the rest of this section, we apply the filter bank in Example 1 to a hexagonally sampled image in the left part of Fig. 6. This is a part of the hexagonal image re-sampled from a 512×512 squarely sampled image Lena by the bilinear interpolation in [6]. The decomposed images (when $M = M_1$) with the lowpass filter p and highpass filters $q^{(1)}, q^{(2)}$ are shown on the right of Fig. 6 and in Fig. 7 respectively. These images are rotated 30° with respect to the original image.

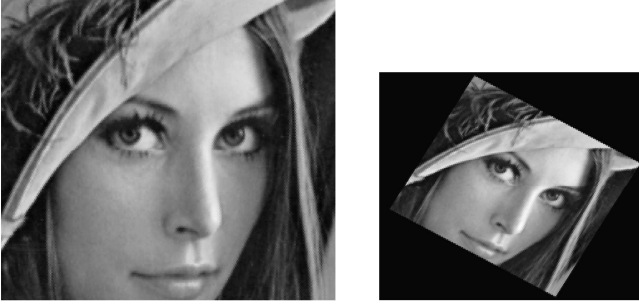


Fig. 6. Left: Original (hexagonal) image; Right: Decomposed image with lowpass filter p

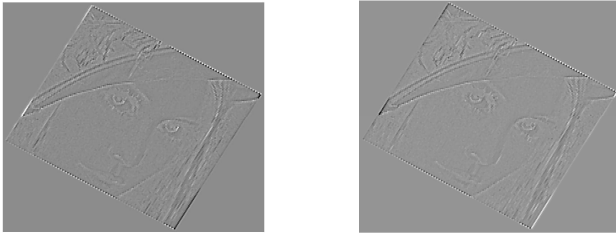


Fig. 7. Decomposed images with highpass filters $q^{(1)}$ (left) and $q^{(2)}$ (right)

IV. BIORTHOGONAL $\sqrt{3}$ -REFINEMENT WAVELETS WITH 6-FOLD SYMMETRY

In this section we consider the construction of biorthogonal $\sqrt{3}$ -refinement FIR filter banks with 6-fold symmetry and the associated wavelets. In §IV.A, we present a characterization of symmetric filter banks. In §IV.B, we provide a family of 6-fold symmetric biorthogonal $\sqrt{3}$ -refinement FIR filter banks and discuss the construction of the associated wavelets.

A. 6-fold axial symmetry

Let

$$L_0 = \begin{bmatrix} 0 & 1 \\ 1 & 0 \end{bmatrix}, L_1 = \begin{bmatrix} 1 & 0 \\ 1 & -1 \end{bmatrix}, L_2 = \begin{bmatrix} 1 & -1 \\ 0 & -1 \end{bmatrix} \\ L_3 = -L_0, L_4 = -L_1, L_5 = -L_2. \quad (23)$$

Then for a j , $0 \leq j \leq 5$, $\{p_k\}$ is symmetric around the symmetry axis S_j in Fig. 5 if and only if $p_{L_j k} = p_k$. Denote

$$R_1 = \begin{bmatrix} 0 & 1 \\ -1 & 1 \end{bmatrix}.$$

Then $\{p_{R_1 k}\}$ is the $\pi/3$ (anticlockwise) rotation of $\{p_k\}$. Furthermore, from the fact

$$L_j = (R_1)^j L_0, \quad 0 \leq j \leq 5,$$

we know when we discuss the 6-fold axial symmetry of a filter bank, we need only consider L_0, R_1 instead of all $L_j, 0 \leq j \leq 5$.

Proposition 1: A filter bank $\{p, q^{(1)}, q^{(2)}\}$ has 6-fold axial symmetry if and only if it satisfies

$$[p, q^{(1)}, q^{(2)}]^T (R_1^{-T} \omega) = N_1(\omega) [p, q^{(1)}, q^{(2)}]^T (\omega) \quad (24)$$

$$[p, q^{(1)}, q^{(2)}]^T (L_0 \omega) = N_2(\omega) [p, q^{(1)}, q^{(2)}]^T (\omega), \quad (25)$$

where

$$N_1(\omega) = \begin{bmatrix} 1 & 0 & 0 \\ 0 & 0 & e^{-i(2\omega_1 + \omega_2)} \\ 0 & e^{i(2\omega_1 + \omega_2)} & 0 \end{bmatrix}, \quad (26) \\ N_2(\omega) = \begin{bmatrix} 1 & 0 & 0 \\ 0 & e^{i(\omega_1 - \omega_2)} & 0 \\ 0 & 0 & e^{-i(\omega_1 - \omega_2)} \end{bmatrix}.$$

Proof. For a filter bank $\{p, q^{(1)}, q^{(2)}\}$, let $h^{(1)}(\omega) = e^{i\omega_1} q^{(1)}(\omega)$, $h^{(2)}(\omega) = e^{-i\omega_1} q^{(2)}(\omega)$. Then with the fact $L_j = R_1^j L_0, 0 \leq j \leq 5$, we know $\{p, q^{(1)}, q^{(2)}\}$ has 6-fold axial symmetry if and only if

$$p(R_1^{-T} \omega) = p(L_0 \omega) = p(\omega), \quad (27)$$

$$h^{(1)}((R_1^{-T})^2 \omega) = h^{(1)}((R_1^{-T})^4 \omega) \\ = h^{(1)}(L_0 \omega) = h^{(1)}(\omega), \quad (28)$$

$$h^{(2)}(-\omega) = h^{(1)}(\omega). \quad (29)$$

Observe that $R_1^3 = -I_2$. This fact and (28) and (29) lead to

$$h^{(1)}(R_1^{-T} \omega) = h^{(1)}(-(R_1^{-T})^4 \omega) = h^{(1)}(-\omega) = h^{(2)}(\omega), \\ h^{(2)}(R_1^{-T} \omega) = h^{(2)}(-(R_1^{-T})^4 \omega) = h^{(1)}((R_1^{-T})^4 \omega) = h^{(1)}(\omega) \\ h^{(2)}(L_0 \omega) = h^{(1)}(-L_0 \omega) = h^{(1)}(-\omega) = h^{(2)}(\omega).$$

Conversely, one can check that $h^{(1)}(R_1^{-T} \omega) = h^{(2)}(\omega)$, $h^{(2)}(R_1^{-T} \omega) = h^{(1)}(\omega)$ and $h^{(2)}(L_0 \omega) = h^{(1)}(\omega)$ imply (28) and (29). Therefore, $\{p, q^{(1)}, q^{(2)}\}$ has 6-fold axial symmetry if and only if

$$[p, h^{(1)}, h^{(2)}]^T (R_1^{-T} \omega) = [p, h^{(2)}, h^{(1)}]^T (\omega), \quad (30)$$

$$[p, h^{(1)}, h^{(2)}]^T (L_0 \omega) = [p, h^{(1)}, h^{(2)}]^T (\omega). \quad (31)$$

With $h^{(1)}(\omega) = e^{i\omega_1} q^{(1)}(\omega)$, $h^{(2)}(\omega) = e^{-i\omega_1} q^{(2)}(\omega)$, one can easily show that (24) and (25) are equivalent to (30) and (31). Hence, $\{p, q^{(1)}, q^{(2)}\}$ has 6-fold axial symmetry if and only if (24) and (25) hold, as desired. \diamond

Let $M = M_1$. For an FIR filter bank $\{p, q^{(1)}, q^{(2)}\}$, let $V(\omega)$ be its polyphase matrix (with $M = M_1$) defined by (19). Based on Proposition 1, we reach the following proposition which gives the characterization of the 6-fold axial symmetry of a filter bank in terms of the corresponding polyphase matrix.

Proposition 2: An FIR filter bank $\{p, q^{(1)}, q^{(2)}\}$ has 6-fold axial symmetry if and only if its polyphase matrix $V(\omega)$ (with dilation matrix $M = M_1$) satisfies

$$V(R_1^{-T}\omega) = N_0(\omega)V(\omega)N_0(\omega), \quad (32)$$

$$V(L_0\omega) = J_0V(\omega)J_0, \quad (33)$$

where

$$N_0(\omega) = \begin{bmatrix} 1 & 0 & 0 \\ 0 & 0 & e^{-i\omega_1} \\ 0 & e^{i\omega_1} & 0 \end{bmatrix}, \quad J_0 = \begin{bmatrix} 1 & 0 & 0 \\ 0 & 0 & 1 \\ 0 & 1 & 0 \end{bmatrix}. \quad (34)$$

Proof. By the definition of $V(\omega)$, we have

$$\begin{aligned} [p, q^{(1)}, q^{(2)}](R_1^{-T}\omega) &= (1/\sqrt{3})V(M^T R_1^{-T}\omega)I_0(R_1^{-T}\omega) \\ &= (1/\sqrt{3})V(M^T R_1^{-T}\omega)N_1(\omega)I_0(\omega). \end{aligned}$$

Thus (24) is equivalent to

$$V(M^T R_1^{-T}\omega)N_1(\omega)I_0(\omega) = N_1(\omega)V(M^T\omega)I_0(\omega),$$

or equivalently,

$$V(M^T R_1^{-T}\omega)N_1(\omega) = N_1(\omega)V(M^T\omega).$$

The fact $M^T R_1^{-T} = R_1^{-T} M^T$ ($M = M_1$) leads to that the above equality is

$$V(R_1^{-T} M^T \omega)N_1(\omega) = N_1(\omega)V(M^T \omega),$$

or,

$$V(R_1^{-T}\omega) = N_1(M^{-T}\omega)V(\omega)N_1(M^{-T}\omega),$$

which is (32) because of the fact $N_1(M^{-T}\omega) = N_0(\omega)$.

Similarly as above, we have that (25) is equivalent to

$$V(M^T L_0\omega) = N_2(\omega)V(M^T\omega)N_2(\omega)^{-1}.$$

From $M^T L_0 = R_1^{-T} L_0 M^T$ (when $M = M_1$), we know that the above equality is

$$V(R_1^{-T} L_0 M^T \omega) = N_2(\omega)V(M^T \omega)N_2(\omega)^{-1},$$

or,

$$V(R_1^{-T} L_0 \omega) = N_2(M^{-T}\omega)V(\omega)N_2(M^{-T}\omega)^T,$$

which in turn is equivalent to (under the assumption (32))

$$\begin{aligned} V(L_0\omega) &= N_0(L_0\omega)V(R_1^{-T} L_0\omega)(L_0\omega) \\ &= N_0(L_0\omega)N_2(M^{-T}\omega)V(\omega)N_2(M^{-T}\omega)^T N_0(L_0\omega)^{-1} \\ &= J_0V(\omega)J_0. \end{aligned}$$

Therefore, (24) and (25) are equivalent to (32) and (33). \diamond

In the next subsection, based on the characterization in Proposition 2 for the 6-fold symmetry of filter banks, we provide a family of biorthogonal FIR filter banks with such a type of symmetry.

B. Biorthogonal $\sqrt{3}$ -refinement wavelets

In this subsection we use the notations: $x = e^{-i\omega_1}$, $y = e^{-i\omega_2}$. Thus an FIR filter $p(\omega)$ can be written as a polynomial of x, y . Denote

$$W(\omega) = \begin{bmatrix} d + c(x + xy + y + \frac{1}{x} + \frac{1}{xy} + \frac{1}{y}) & a(1 + \frac{1}{x} + y) & a(1 + x - \frac{1}{x} - y) \\ \frac{c}{2a}(1 + x + \frac{1}{y}) & 1 & 0 \\ \frac{c}{2a}(1 + \frac{1}{x} + y) & 0 & 1 \end{bmatrix} \quad (35)$$

where a, c, d are constants with $a \neq 0, d \neq 3c$. Next we use $W(\omega)$ to build a block structure of biorthogonal FIR filter banks with 6-fold symmetry. This filter bank $\{p, q^{(1)}, q^{(2)}\}$ has 6-fold axial symmetry. (One may verify directly that its polyphase matrix $W(\omega)$ satisfies (32) and (33)). If $a = 1/3, d = 2/3, c = 1/(18)$, then the corresponding $\{p_k\}$ is the subdivision mask constructed in [23].

Except for the property that $W(\omega)$ produces a 6-fold symmetry filter bank, $W(\omega)$ has another important property: the determinant of $W(\omega)$ is $d - 3c$, a nonzero constant. Thus, the inverse of $W(\omega)$ is a matrix whose entries are also polynomials of x, y . More precisely, $\widetilde{W}(\omega) = (W(\omega)^{-1})^*$ is

$$\begin{aligned} \widetilde{W}(\omega) &= \frac{1}{d-3c} \times \\ &\begin{bmatrix} 1 & -\frac{c}{2a}(1 + \frac{1}{x} + y) & -\frac{c}{2a}(1 + x - \frac{1}{x} - y) \\ -a(1 + x + \frac{1}{y}) & d - \frac{3}{2}c + \frac{c}{2}(x + xy + y + \frac{1}{x} + \frac{1}{xy} + \frac{1}{y}) & 0 \\ -a(1 + \frac{1}{x} + y) & \frac{c}{2}(1 + \frac{1}{x} + y)^2 & d - \frac{3}{2}c + \frac{c}{2}(1 + x - \frac{1}{x} - y)^2 \end{bmatrix} \end{aligned} \quad (36)$$

Hence, $\{p, q^{(1)}, q^{(2)}\}$ has a biorthogonal FIR filter bank $\{\widetilde{p}, \widetilde{q}^{(1)}, \widetilde{q}^{(2)}\}$ defined by $[\widetilde{p}(\omega), \widetilde{q}^{(1)}(\omega), \widetilde{q}^{(2)}(\omega)]^T = \widetilde{W}(M^T\omega)I_0(\omega)$. In addition, one can check directly (or from the fact $W(\omega)$ satisfies (32) and (33)) that $\widetilde{W}(\omega)$ satisfies (32) and (33). Thus, $\{\widetilde{p}, \widetilde{q}^{(1)}, \widetilde{q}^{(2)}\}$ also has 6-fold axial symmetry. More general, we have the following result.

Theorem 2: Suppose FIR filter banks $\{p, q^{(1)}, q^{(2)}\}$ and $\{\widetilde{p}, \widetilde{q}^{(1)}, \widetilde{q}^{(2)}\}$ are given by

$$\begin{aligned} [p(\omega), q^{(1)}(\omega), q^{(2)}(\omega)]^T &= U_n(M^T\omega) \cdots U_0(M^T\omega)I_0(\omega), \\ [\widetilde{p}(\omega), \widetilde{q}^{(1)}(\omega), \widetilde{q}^{(2)}(\omega)]^T &= (1/3)\widetilde{U}_n(M^T\omega) \cdots \widetilde{U}_0(M^T\omega)I_0(\omega) \end{aligned} \quad (37)$$

where $n \in \mathbf{Z}_+$, $I_0(\omega)$ is defined by (14), each $U_k(\omega)$ is a $W(\omega)$ in (35) or a $\widetilde{W}(\omega)$ in (36) for some parameters a_k, b_k, d_k , and $\widetilde{U}_k(\omega) = (U_k(\omega)^{-1})^*$ is the corresponding $\widetilde{W}(\omega)$ in (36) or $W(\omega)$ in (35), then $\{p, q^{(1)}, q^{(2)}\}$ and $\{\widetilde{p}, \widetilde{q}^{(1)}, \widetilde{q}^{(2)}\}$ are biorthogonal FIR filter bank with 6-fold axial symmetry.

Next we consider the construction of biorthogonal $\sqrt{3}$ -refinement wavelets based on the symmetric biorthogonal FIR filter banks given in (37). When we construct biorthogonal wavelets, we will intently construct the synthesis scaling function $\widetilde{\phi}$ to have a higher smoothness order. Smoothness of $\widetilde{\phi}$ is in general more important than that for ϕ since certain smoothness of $\widetilde{\phi}$ is required to assure the reconstructed image/surface to have nice visual quality.

First, we consider the filter banks given by (37) with $n = 0$. Let $[p(\omega), q^{(1)}(\omega), q^{(2)}(\omega)]^T = \widetilde{W}_0(M^T\omega)I_0(\omega)$ and $[\widetilde{p}(\omega), \widetilde{q}^{(1)}(\omega), \widetilde{q}^{(2)}(\omega)]^T = (1/3)\widetilde{W}_0(M^T\omega)I_0(\omega)$, where $\widetilde{W}_0(\omega)$ and $W_0(\omega)$ are given by (36) and (35) respectively for

some parameters a_0, c_0, d_0 . By solving the system of equations for sum rule order 1 of $\tilde{p}(\omega)$, we have

$$a_0 = 1/3, d_0 = 1 - 6c_0. \quad (38)$$

The resulting $\tilde{p}(\omega)$ actually has sum rule order 2 (the conditions in (22) for $\tilde{p}(\omega)$ with $(\alpha_1, \alpha_2) = (1, 0)$ and $(\alpha_1, \alpha_2) = (0, 1)$ are automatically satisfied because of the symmetry of $\tilde{p}(\omega)$). If in addition, we choose $c_0 = 1/(18)$, then $\tilde{p}(\omega)$ has sum rule order 3. This $\tilde{p}(\omega)$ is the subdivision mask in [23]. However, in this case the resulting $p(\omega)$ does not have sum rule order 1, which implies the corresponding scaling function ϕ is not in $L^2(\mathbb{R}^2)$. With a_0, d_0 given by (38) for some c_0 , by solving the system of equations for sum rule order 1 of $p(\omega)$, we have $c_0 = -2/9$. However, in this case the corresponding $\tilde{\phi}$ is not in $L^2(\mathbb{R}^2)$. Thus, the filter banks in (37) with $n = 0$ cannot generate scaling functions ϕ and $\tilde{\phi}$ such that both of them are in $L^2(\mathbb{R}^2)$, and hence, these filter banks cannot generate biorthogonal wavelets.

Example 3: Let $\{p, q^{(1)}, q^{(2)}\}$ and $\{\tilde{p}, \tilde{q}^{(1)}, \tilde{q}^{(2)}\}$ be the biorthogonal filter banks given by (37) for $n = 1$ with

$$\begin{aligned} [p(\omega), q^{(1)}(\omega), q^{(2)}(\omega)]^T &= W_1(M^T \omega) \tilde{W}_0(M^T \omega) I_0(\omega), \\ [\tilde{p}(\omega), \tilde{q}^{(1)}(\omega), \tilde{q}^{(2)}(\omega)]^T &= (1/3) \tilde{W}_1(M^T \omega) W_0(M^T \omega) I_0(\omega), \end{aligned}$$

where $\tilde{W}_0(\omega)$, $\tilde{W}_1(\omega)$, and $W_0(\omega)$, $W_1(\omega)$ are given by (36) and (35) for some parameters a_0, c_0, d_0 and a_1, c_1, d_1 .

We notice that the smoothness of $\phi, \tilde{\phi}$ is independent of some parameters, e.g. d_1 . In the following we let $d_1 = 0$. If

$$\begin{aligned} a &= c_1(1 - 2a_1)/(2a_1), \quad c = c_1(9a_1 - 1)(1 - 2a_1)/(3a_1), \\ d &= c_1(36a_1^2 + 2a_1 - 1)/a_1, \end{aligned}$$

then both $p(\omega)$ and $\tilde{p}(\omega)$ have sum rule order 2. If we choose $a_1 = 8/(81)$, $c_1 = 1$, then the resulting ϕ is in $W^{0.1289}$, and $\tilde{\phi}$ in $W^{1.3474}$; while if we choose $a_1 = 1/(10)$, $c_1 = 1$, then the resulting $\phi \in W^{0.0911}$, and $\tilde{\phi} \in W^{1.3777}$. One may choose other values for a_1, c_1 such that the resulting $\tilde{\phi}$ is smoother. But $\tilde{\phi}$ can only gain very slight increments of smoothness order if its dual ϕ is in $L^2(\mathbb{R}^2)$. \diamond

Example 4: Let $\{p, q^{(1)}, q^{(2)}\}$ and $\{\tilde{p}, \tilde{q}^{(1)}, \tilde{q}^{(2)}\}$ be the biorthogonal filter banks given by (37) for $n = 1$ with

$$\begin{aligned} [p(\omega), q^{(1)}(\omega), q^{(2)}(\omega)]^T &= \tilde{W}_1(M^T \omega) \tilde{W}_0(M^T \omega) I_0(\omega), \\ [\tilde{p}(\omega), \tilde{q}^{(1)}(\omega), \tilde{q}^{(2)}(\omega)]^T &= (1/3) W_1(M^T \omega) W_0(M^T \omega) I_0(\omega), \end{aligned}$$

where $\tilde{W}_0(\omega)$, $\tilde{W}_1(\omega)$, and $W_0(\omega)$, $W_1(\omega)$ are given by (36) and (35) for some parameters a_0, c_0, d_0 and a_1, c_1, d_1 . In this case, \tilde{p} has a larger filter length than p . We will use $\{\tilde{p}, \tilde{q}^{(1)}, \tilde{q}^{(2)}\}$ as the analysis filter bank (for multiresolution decomposition algorithm) and use $\{p, q^{(1)}, q^{(2)}\}$ as the synthesis filter bank (for multiresolution reconstruction algorithm). Hence, we will construct ϕ to be smoother than its dual $\tilde{\phi}$.

If

$$\begin{aligned} a_1 &= \frac{3a - d - 6c}{3(3c - d)}, \quad c_1 = \frac{(3c + 2a)(6c + d - 3a)}{9a(3c - d)(6c + 6a + d)}, \\ d_1 &= \frac{3c - 18acc_1 + 6adc_1 - a}{a(3c - d)}, \end{aligned}$$

then both $p(\omega)$ and $\tilde{p}(\omega)$ have sum rule order 2. If in addition, $d = -(3a)/(4a^2 + 11ca + 9c^2)$, then $p(\omega)$ has sum rule order 3. There are two free parameters a, c . (We cannot choose a, c further such that $\tilde{p}(\omega)$ also has sum rule order 3.) With many choices of different values for a, c , the resulting $\phi \in C^1$ while $\tilde{\phi}$ has certain smoothness order. For example, if we choose $a = -1/3, c = 2$, then the corresponding $\tilde{\phi} \in W^{0.0758}$ and $\phi \in W^{2.3426}$; with $a = -1/3, c = 1$, the resulting $\tilde{\phi} \in W^{0.3284}$ and $\phi \in W^{2.2354}$; and if

$$a = -1/3, \quad c = 1/2, \quad (39)$$

then $\tilde{\phi} \in W^{1.0507}$, $\phi \in W^{1.9145}$. The corresponding biorthogonal filter banks, denoted as $\text{Bio}_{(6,8)}$, when a, c are given by (39) are provided in the long version of this paper. In this case, the corresponding d, a_1, c_1, d_1 defined above for sum rule orders are

$$d = \frac{31}{4}, \quad a_1 = \frac{47}{75}, \quad c_1 = \frac{94}{1575}, \quad d_1 = \frac{274}{525} \cdot \diamond$$

Except for $W(\omega)$ and $\tilde{W}(\omega)$, we may use other matrices as blocks to build the biorthogonal filter banks. For example, we may use

$$Z(\omega) = \begin{bmatrix} 1 & e_0(1 + \frac{1}{x} + y) + e_1(xy + \frac{1}{xy} + \frac{y}{x}) & e_0(1 + x + \frac{1}{y}) + e_1(x + \frac{1}{x} + y) & 0 \\ 0 & 1 & 0 & 0 \\ 0 & 0 & 0 & 1 \end{bmatrix} \quad (40)$$

where e_0, e_1 are constants. For $Z(\omega)$ defined by (40), $\tilde{Z}(\omega) = (Z(\omega)^{-1})^*$ is given by

$$\tilde{Z}(\omega) = \begin{bmatrix} 1 & 0 & 0 \\ -e_0(1 + x + \frac{1}{y}) - e_1(xy + \frac{1}{xy} + \frac{x}{y}) & 1 & 0 \\ -e_0(1 + \frac{1}{x} + y) - e_1(1 + \frac{1}{xy} + \frac{y}{x}) & 0 & 1 \end{bmatrix} \quad (41)$$

Clearly both $Z(\omega)$ and $\tilde{Z}(\omega)$ satisfy (32) and (33). Thus if $\{p, q^{(1)}, q^{(2)}\}$ and $\{\tilde{p}, \tilde{q}^{(1)}, \tilde{q}^{(2)}\}$ are given by (37) for some $n \in \mathbf{Z}_+$ with each $U_k(\omega)$ is a $W(\omega)$ in (35), a $\tilde{W}(\omega)$ in (36), a $Z(\omega)$ in (40), or a $\tilde{Z}(\omega)$ in (41), and $\tilde{U}_k(\omega) = (U_k(\omega)^{-1})^*$ is the corresponding $\tilde{W}(\omega)$ ($W(\omega)$, $\tilde{Z}(\omega)$, or $Z(\omega)$ accordingly), then $\{p, q^{(1)}, q^{(2)}\}$ and $\{\tilde{p}, \tilde{q}^{(1)}, \tilde{q}^{(2)}\}$ are biorthogonal FIR filter bank with 6-fold axial symmetry. Next, as an example, we show how $W(\omega)$ and $Z(\omega)$ reach some interesting biorthogonal filter banks, including those constructed in [40] (for regular nodes).

Example 5: Let $\{p, q^{(1)}, q^{(2)}\}$ and $\{\tilde{p}, \tilde{q}^{(1)}, \tilde{q}^{(2)}\}$ be the biorthogonal filter banks given by

$$\begin{aligned} [p(\omega), q^{(1)}(\omega), q^{(2)}(\omega)]^T &= Z(M^T \omega) \tilde{W}(M^T \omega) I_0(\omega), \\ [\tilde{p}(\omega), \tilde{q}^{(1)}(\omega), \tilde{q}^{(2)}(\omega)]^T &= (1/3) \tilde{Z}(M^T \omega) W(M^T \omega) I_0(\omega), \end{aligned}$$

where $W(\omega)$, $\tilde{W}(\omega)$, $Z(\omega)$, and $\tilde{Z}(\omega)$ are given by (35), (36), (40), and (41) for some parameters a, b, d and e_0, e_1 .

By solving the system of equations for sum rule order 1 of $\tilde{p}(\omega)$, we have

$$a = 1/3, \quad d = 1 - 6c. \quad (42)$$

Again, the resulting \tilde{p} actually has sum rule order 2 because of the symmetry of \tilde{p} . Then by solving the system of equations

for sum rule order 1 of $p(\omega)$, we have

$$e_0 = 1/9 + c/2 - e_1. \quad (43)$$

With (43), the resulting p also has sum rule order 2 because of its symmetry. If in addition,

$$e_1 = -5/(81) - c/3 - c^2, \quad (44)$$

then $p(\omega)$ has sum rule order 3.

If $c = 1/(18)$ (and a, d are given in (42)), then the resulting $\tilde{p}(\omega)$ has sum rule order 3. As mentioned above, this $\tilde{p}(\omega)$ is the subdivision mask in [23] for surface subdivision. It was calculated in [25] that the corresponding $\tilde{\phi}$ is in $W^{2.9360}$. However, we find that for $c = 1/(18)$, for any value e_1 (with e_0 given in (43)), the corresponding ϕ is not in $L^2(\mathbb{R}^2)$. (Paper [40] chooses two groups of values: $c = 1/(18)$, $e_0 = 0.229537$, $e_1 = 0$, and $c = 1/(18)$, $e_0 = 0.279682$, $e_1 = -0.142329$.) In the following we may choose other values for c . For example, if we choose c as (with a, d, e_0, e_1 defined by (42)-(44)) $c = 1/(37)$, then the corresponding $\phi \in W^{0.0027}$ and $\tilde{\phi} \in W^{1.9344}$; and if $c = 2/(81)$, then the corresponding $\phi \in W^{0.0540}$ and $\tilde{\phi} \in W^{1.9184}$. If we remove the requirement (44) for sum rule order 3 of $p(\omega)$, then with $c = 1/(27)$, $e_1 = -1/(10)$, the resulting $\phi \in W^{0.0104}$ and $\tilde{\phi} \in W^{1.9801}$. We check numerically that all the resulting scaling functions $\tilde{\phi}$ are in C^1 . The resulting biorthogonal filter banks, denoted as $\text{Bio}_{(8,4)}$, corresponding to $c = 1/(27)$, $e_1 = -1/(10)$ are provided in the long version of this paper. \diamond

V. CONCLUSION

In this paper we introduce $\sqrt{3}$ -refinement orthogonal hexagonal filter banks with 2-fold rotational symmetry and biorthogonal hexagonal filter banks with 6-fold axial symmetry. We obtain block structures of these filter banks. Based on these block structures, we construct compactly supported orthogonal and biorthogonal $\sqrt{3}$ -refinement hexagonal wavelets. Our future work is to apply these hexagonal filter banks and wavelets for hexagonal data processing applications such as image enhancement and edge detection. We will also compare the experiment results obtained by the $\sqrt{3}$ -refinement wavelets constructed in this paper with those obtained by the dyadic and $\sqrt{7}$ -refinement wavelets.

Acknowledgments. The author thanks Dale K. Pounds for his kind help to create Figs. 6-7.

REFERENCES

- [1] D.P. Petersen and D. Middleton, "Sampling and reconstruction of wave-number-limited functions in N-dimensional Euclidean spaces", *Information and Control*, vol. 5, no. 4, pp. 279-323, Dec. 1962.
- [2] R.M. Mersereau, "The processing of hexagonal sampled two-dimensional signals", *Proc. IEEE*, vol. 67, no. 6, pp. 930-949, Jun. 1979.
- [3] R.C. Staunton and N. Storey, "A comparison between square and hexagonal sampling methods for pipeline image processing", in *Proc. of SPIE Vol. 1194, Optics, Illumination, and Image Sensing for Machine Vision IV*, 1990, pp. 142-151.
- [4] G. Tirunelveli, R. Gordon, and S. Pistorius, "Comparison of square-pixel and hexagonal-pixel resolution in image processing", in *Proceedings of the 2002 IEEE Canadian Conference on Electrical and Computer Engineering*, vol. 2, May 2002, pp. 867-872.

- [5] D. Van De Ville, T. Blu, M. Unser, W. Philips, I. Lemahieu, and R. Van de Walle, "Hex-splines: a novel spline family for hexagonal lattices", *IEEE Trans. Image Proc.*, vol. 13, no. 6, pp. 758-772, Jun. 2004.
- [6] L. Middleton and J. Sivaswamy, *Hexagonal Image Processing: A Practical Approach*, Springer, 2005.
- [7] X.J. He and W.J. Jia, "Hexagonal structure for intelligent vision", in *Proceedings of the 2005 First International Conference on Information and Communication Technologies*, Aug. 2005, pp. 52-64.
- [8] X.Q. Zheng, "Efficient Fourier Transforms on Hexagonal Arrays", Ph.D. Dissertation, University of Florida, 2007.
- [9] R.C. Staunton, "The design of hexagonal sampling structures for image digitization and their use with local operators", *Image and Vision Computing*, vol. 7, no. 3, pp. 162-166, Aug. 1989.
- [10] L. Middleton and J. Sivaswamy, "Edge detection in a hexagonal-image processing framework", *Image and Vision Computing*, vol. 19, no. 14, pp. 1071-1081, Dec. 2001.
- [11] A.F. Laine, S. Schuler, J. Fan, and W. Huda, "Mammographic feature enhancement by multiscale analysis", *IEEE Trans. Med. Imaging*, vol. 13, no. 4, pp. 725-740, Dec. 1994.
- [12] A.F. Laine and S. Schuler, "Hexagonal wavelet representations for recognizing complex annotations", in *Proceedings of the IEEE Conference on Computer Vision and Pattern Recognition*, Seattle, WA, Jun. 1994, pp. 740-745.
- [13] A.P. Fitz and R. Green, "Fingerprint classification using hexagonal fast Fourier transform", *Pattern Recognition*, vol. 29, no. 10, pp. 1587-1597, 1996.
- [14] S. Periaswamy, "Detection of microcalcification in mammograms using hexagonal wavelets", M.S. thesis, Dept. of Computer Science, Univ. of South Carolina, Columbia, SC, 1996.
- [15] R.C. Staunton, "One-pass parallel hexagonal thinning algorithm", *IEEE Proceedings on Vision, Image and Signal Processing*, vol. 148, no. 1, pp. 45-53, Feb. 2001.
- [16] A. Camps, J. Bara, I.C. Sanahuja, and F. Torres, "The processing of hexagonally sampled signals with standard rectangular techniques: application to 2-D large aperture synthesis interferometric radiometers", *IEEE Trans. Geoscience and Remote Sensing*, vol. 35, no. 1, pp. 183-190, Jan. 1997.
- [17] E. Anterrieu, P. Waldteufel, and A. Lannes, "Apodization functions for 2-D hexagonally sampled synthetic aperture imaging radiometers", *IEEE Trans. Geoscience and Remote Sensing*, vol. 40, no. 12, pp. 2531-2542, Dec. 2002.
- [18] F. Vipiana, G. Vecchi, and M. Sabbadini, "A multiresolution approach to contoured-beam antennas", *IEEE Trans. Antennas and Propagation*, vol. 55, no. 3, pp. 684-697, Mar. 2007.
- [19] D. White, A.J. Kimberling, and W.S. Overton, "Cartographic and geometric components of a global sampling design for environmental monitoring", *Cartography and Geographic Information Systems*, vol. 19, no. 1, pp. 5-22, 1992.
- [20] K. Sahr, D. White, and A.J. Kimberling, "Geodesic discrete global grid systems", *Cartography and Geographic Information Science*, vol. 30, no. 2, pp. 121-134, Apr. 2003.
- [21] M.J.E. Golay, "Hexagonal parallel pattern transformations", *IEEE Trans. Computers*, vol. 18, no. 8, pp. 733-740, Aug. 1969.
- [22] P.J. Burt, "Tree and pyramid structures for coding hexagonally sampled binary images", *Computer Graphics and Image Proc.*, vol. 14, no. 3, pp. 271-80, 1980.
- [23] L. Kobbelt, " $\sqrt{3}$ -subdivision", in *SIGGRAPH Computer Graphics Proceedings*, pp. 103-112, 2000.
- [24] U. Labsik and G. Greiner, "Interpolatory $\sqrt{3}$ -subdivision", *Computer Graphics Forum*, vol. 19, no. 3, pp. 131-138, Sep. 2000.
- [25] Q.T. Jiang and P. Oswald, "Triangular $\sqrt{3}$ -subdivision schemes: the regular case", *J. Comput. Appl. Math.*, vol. 156, no. 1, pp. 47-75, Jul. 2003.
- [26] Q.T. Jiang, P. Oswald, and S.D. Riemenschneider, " $\sqrt{3}$ -subdivision schemes: maximal sum rules orders", *Constr. Approx.*, vol. 19, no. 3, pp. 437-463, 2003.
- [27] P. Oswald and P. Schröder, "Composite primal/dual $\sqrt{3}$ -subdivision schemes", *Comput. Aided Geom. Design*, vol. 20, no. 3, pp. 135-164, Jun. 2003.
- [28] C.K. Chui and Q.T. Jiang, "Surface subdivision schemes generated by refinable bivariate spline function vectors", *Appl. Comput. Harmonic Anal.*, vol. 15, no. 2, pp. 147-162, Sep. 2003.
- [29] C.K. Chui and Q.T. Jiang, "Matrix-valued symmetric templates for interpolatory surface subdivisions, I: regular vertices", *Appl. Comput. Harmonic Anal.*, vol. 19, no. 3, pp. 303-339, Nov. 2005.

- [30] E. Simoncelli and E. Adelson, "Non-separable extensions of quadrature mirror filters to multiple dimensions", *Proceedings of the IEEE*, vol. 78, no. 4, pp. 652–664, Apr. 1990.
- [31] H. Xu, W.-S. Lu, and A. Antoniou, "A new design of 2-D non-separable hexagonal quadrature-mirror-filter banks", in *Proc. CCECE*, Vancouver, Sep. 1993, pp. 35–38.
- [32] A. Cohen and J.-M. Schlenker, "Compactly supported bidimensional wavelets bases with hexagonal symmetry", *Constr. Approx.*, vol. 9, no. 2/3, pp. 209–236, Jun. 1993.
- [33] J.D. Allen, "Coding transforms for the hexagon grid", Ricoh Calif. Research Ctr., Technical Report CRC-TR-9851, Aug. 1998.
- [34] M. Bertram, "Biorthogonal Loop-subdivision wavelets", *Computing*, vol. 72, no. 1-2, pp. 29–39, Apr. 2004.
- [35] J.D. Allen, "Perfect reconstruction filter banks for the hexagonal grid", In *Fifth International Conference on Information, Communications and Signal Processing 2005*, Dec. 2005, pp. 73–76.
- [36] Q.T. Jiang, "FIR filter banks for hexagonal data processing", *IEEE Trans. Image Proc.*, vol. 17, no. 9, pp. 1512–1521, Sep. 2008.
- [37] Q.T. Jiang, "Orthogonal and biorthogonal FIR hexagonal filter banks with sixfold symmetry", *IEEE Trans. Signal Proc.*, vol. 52, no. 12, pp. 5861–5873, Dec. 2008.
- [38] Documents of Pyxis Innovation Inc., <http://www.pyxisinnovation.com>.
- [39] L. Condat, B. Forster-Heinlein, and D. Van De Ville, "A new family of rotation-covariant wavelets on the hexagonal lattice", in *Proc. of the SPIE Optics and Photonics 2007 Conference on Mathematical Methods: Wavelet XII*, San Diego CA, USA, August, 2007, vol. 6701, pp. 67010B-1/67010B-9.
- [40] H.W. Wang, K.H. Qin, and H.Q. Sun, " $\sqrt{3}$ -subdivision-based biorthogonal wavelets", *IEEE Trans. Visualization and Computer Graphics*, vol. 13, no. 5, pp. 914–925, Sep./Oct. 2007.
- [41] D. Van De Ville, T. Blu, and M. Unser, "Isotropic polyharmonic B-splines: scaling functions and wavelets", *IEEE Trans. Image Proc.*, vol. 14, no. 11, pp. 1798–1813, Nov. 2005.
- [42] A. Cohen and I. Daubechies, "A stability criterion for biorthogonal wavelet bases and their related subband coding scheme", *Duke Math. J.*, vol. 68, no. 2, pp. 313–335, 1992.
- [43] R.Q. Jia, "Convergence of vector subdivision schemes and construction of biorthogonal multiple wavelets", In *Advances in Wavelets*, Springer-Verlag, Singapore, 1999, pp. 199–227.
- [44] C.K. Chui and Q.T. Jiang, "Multivariate balanced vector-valued refinable functions", in *Modern Development in Multivariate Approximation*, ISNM 145, Birkhäuser Verlag, Basel, 2003, pp. 71–102.
- [45] C. de Boor, K. Höllig, and S. Riemenschnieder, *Box splines*, Springer-Verlag, New York, 1993.
- [46] R.Q. Jia and S.R. Zhang, "Spectral properties of the transition operator associated to a multivariate refinement equation", *Linear Algebra Appl.*, vol. 292, no. 1, pp. 155–178, May 1999.
- [47] R.Q. Jia and Q.T. Jiang, "Spectral analysis of transition operators and its applications to smoothness analysis of wavelets", *SIAM J. Matrix Anal. Appl.*, vol. 24, no. 4, pp. 1071–1109, 2003.

PLACE
PHOTO
HERE

Qingtang Jiang received the B.S. and M.S. degrees from Hangzhou University, Hangzhou, China, in 1986 and 1989, respectively, and the Ph.D. degree from Peking University, Beijing, China, in 1992, all in mathematics. He was with Peking University from 1992 to 1995. He was an NSTB postdoctoral fellow and then a research fellow at the National University of Singapore from 1995 to 1999. Before he joined the University of Missouri-St. Louis, in 2002, he held visiting positions at University of Alberta, Canada, and West Virginia University, Morgantown.

He is now a Professor in the Department of Math and Computer Science, University of Missouri-St. Louis. His current research interests include time-frequency analysis, wavelet theory and its applications, filter bank design, signal classification, image processing, and surface subdivision.